Mathematical Modelling and Numerical Simulation with Applications, 2022, 2(2), 108–116

https://www.mmnsa.org
ISSN Online: 2791-8564 / Open Access
https://doi.org/10.53391/mmnsa.2022.009

RESEARCH PAPER

An optimal control strategy and Grünwald-Letnikov finite-difference numerical scheme for the fractional-order COVID-19 model

Ihtisham Ul Haq [1,‡,*], Nigar Ali [1,‡] and Kottakkaran Sooppy Nisar [2,‡]

[1]Department of Mathematics, University of Malakand, Chakdara Dir (L), 18000, Khyber Pakhtunkhwa, Pakistan,
[2]Department of Mathematics, College of Arts and Science, Prince Sattam bin Abdulaziz University, Saudi Arabia

[*]Corresponding Author
[‡]ihtisham0095@gmail.com (Ihtisham Ul Haq); nigaruom@gmail.com (Nigar Ali); n.soopy@psau.edu.sa (Kottakkaran Sooppy Nisar)

Abstract

In this article, a mathematical model of the COVID-19 pandemic with control parameters is introduced. The main objective of this study is to determine the most effective model for predicting the transmission dynamic of COVID-19 using a deterministic model with control variables. For this purpose, we introduce three control variables to reduce the number of infected and asymptomatic or undiagnosed populations in the considered model. Existence and necessary optimal conditions are also established. The Grünwald-Letnikov non-standard weighted average finite difference method (GL-NWAFDM) is developed for solving the proposed optimal control system. Further, we prove the stability of the considered numerical method. Graphical representations and analysis are presented to verify the theoretical results.

Key words: Caputo fractional derivative; optimal control strategy; Grünwald-Letnikov numerical method; stability analysis
AMS 2020 Classification: 92B05; 49K10; 49J15; 65L03; 65L20

1 Introduction

COVID-19 pandemic can be considered as a dangerous infectious disease in the whole world, see [1]. It is transmitted to humans primarily through tiny droplets, or contact with contaminated surfaces. Mathematical modelling of epidemic diseases is very helpful for control strategies to a disease. Recently, a number of interesting papers have been developed regarding the modelling of the coronavirus, see for example [2, 3, 4, 5, 6, 7, 8, 9].

It has recently come to light that Fractional Differential Equations (FDE) can be successfully applied in mathematical modelling in various fields, including epidemics [10]. Fractional Calculus (FC) is a branch of mathematical analysis that deals with the study of fractional-order of derivatives and integral. A dynamical system using fractional-order derivative (FOD) in modeling helps define efficiency, usefulness, and memory as essential properties in many biological mechanisms [11, 12, 13, 14, 15, 16].

Optimal control (OC) theory is a branch of mathematical optimization. It involves investigating the control strategies for a dynamic system in a short time, such as minimizing or maximizing an objective function. Recently, OC theory has been used successfully in many fields, including robotics, aerospace, economics, finance, and management sciences [17, 18, 19]. Especially, the study of epidemiological models is closely related to the study of OC, as vaccination [20], resource allocation [21] and educational campaigns [22]. Caputo and Riemann–Liouville fractional derivatives [23, 24, 25, 26, 27] are the most important definitions of FD. Al-Mekhlafi and Sweilam established important numerical results for FOC [28, 29, 30].

An important contribution to this work is the development of numerical schemes providing approximate solutions for the fractional-order control problems (FOCPs). We discuss the COVID-19 model in [31] with changed fractional operator and parameters. This model was

➤ **Received:** 17.04.2022 ➤ **Revised:** 13.06.2022 ➤ **Accepted:** 20.06.2022 ➤ **Published:** 26.06.2022

modified with three controls $\mathscr{U}_l, \mathscr{U}_q$, and $\mathscr{U}_s$, to decrease the number of the infected, quarantine, and self-isolation. Finally, the numerical simulation is represented in the proposed system.

2 Basic definitions

Definition 1 *We define the Caputo fractional order derivative of the function $\mathscr{P}(t)$ [32]:*

$$ {}_0^c\mathscr{D}_t^\alpha[\mathscr{P}(t)] = \frac{1}{\Gamma(\mathscr{K}-\alpha)} \int_0^t (t-\eta)^{\mathscr{K}-\alpha-1} \mathscr{P}(t)^{(\mathscr{K})}(\eta) d\eta, \tag{1} $$

where, $\mathscr{K} = [\alpha] + 1$ and $[\alpha]$ represents the integral parts of α.

Definition 2 *The discretization of Fractional derivative by the Grünwald–Letnikov approach [33]*

$$ {}_0^c\mathscr{D}_t^\alpha[\mathscr{P}(t)] \mid_{t=t^{\mathscr{K}}} = \frac{1}{\Delta t^\alpha} \left(\mathscr{P}_{\mathscr{K}+1} - \sum_{i=1}^{\mathscr{K}+1} \mathscr{U}_i \mathscr{P}_{\mathscr{K}+1-i} - \mathscr{Y}_{\mathscr{K}+1}\mathscr{P}_0 \right), \tag{2} $$

where, $\mathscr{K} = 1, 2, ..., \mathscr{N}_{\mathscr{K}}$, and the coordinate of each mesh point is $t^{\mathscr{K}} = \mathscr{K}\Delta t, \Delta t = \frac{\mathcal{T}_f}{\mathscr{N}_{\mathscr{K}}}, \mathscr{U}_i = (-1)^{i-1} \begin{pmatrix} \alpha \\ i \end{pmatrix}, \mathscr{U}_1 = \alpha, \mathscr{Y}_i = \frac{i^\alpha}{\Gamma(1-\alpha)}$ and $i = 1, 2, 3, ..., \mathscr{K} + 1$.

Additionally, Let us assume that $0 < \mathscr{U}_{i+1} < \mathscr{U}_i < ... < \mathscr{U}_1 = \alpha < 1, 0 < \mathscr{Y}_{i+1} < \mathscr{Y}_i < ... < \mathscr{Y}_1 = \frac{1}{\Gamma(1-\alpha)}$.

Definition 3 *Let a function $\mathscr{P} : \mathscr{R}^+ \to \mathscr{R}$, the fractional integral is defined by*

$$ {}_0\mathscr{I}_t^\alpha \mathscr{P}(t) = \frac{1}{\Gamma(\alpha)} \int_0^t (t-\eta)^{\alpha-1} \mathscr{P}(\eta) d\eta, $$

where, $\mathscr{K} = [\alpha] + 1$ and $[\alpha]$ represents the integral parts of α.

3 Mathematical model formulation

In this section, we discuss the mathematical model that consists of four compartments of the population which includes susceptible individuals $\mathbb{S}$, asymptomatic infectious $\mathbb{I}$, unreported symptomatic infectious $\mathbb{U}$, and reported symptomatic infectious $\mathbb{R}$. This model was developed in [31]. We modified the model with control variables and then represented it by a system of Caputo fractional derivative:

$$ \begin{cases} {}_0^c\mathscr{D}_t^\alpha[\mathbb{S}] = -(1-\mathscr{U}_l)\,\mathscr{J}(t)\mathbb{S}(t)\left[\mathbb{I}(t) + \mathbb{U}(t)\right] - \mathscr{U}_q\mathbb{S} + \mathscr{U}_s\mathbb{U}, \\ {}_0^c\mathscr{D}_t^\alpha[\mathbb{I}] = (1-\mathscr{U}_l)\,\mathscr{J}(t)\mathbb{S}(t)\left[\mathbb{I}(t) + \mathbb{U}(t)\right] - \beta\mathbb{I}(t), \\ {}_0^c\mathscr{D}_t^\alpha[\mathbb{R}] = \beta_1\mathbb{I}(t) - \mu\mathbb{R}(t) + \mathscr{U}_q\mathbb{S}, \\ {}_0^c\mathscr{D}_t^\alpha[\mathbb{U}] = \beta_2\mathbb{I}(t) - \mu\mathbb{U}(t) - \mathscr{U}_s\mathbb{U}, \end{cases} \tag{3} $$

with the initial conditions $\mathbb{S}(t_0) = \mathbb{S}_0, \mathbb{I}(t_0) = \mathbb{I}_0, \mathbb{R}(t_0) = 0, \mathbb{U}(t_0) \geq 0$, where the function $\mathscr{U}_s, \mathscr{U}_q, \mathscr{U}_l$, are self isolation strategies, quarantine and states lock down, respectively. Table 1 represents the variables and Table 2 shows the descriptions of the model parameters.

Table 1. The variables of system (3)

Variable	Interpretation
$\mathbb{S}$	Susceptible individuals
$\mathbb{I}$	Asymptomatic Infection population
$\mathbb{R}$	Reported symptomatic infected population
$\mathbb{U}$	Unreported symptomatic infected population

Table 2. The parameters of system (3)

Parameter	Biological interpretations
t_0	The time when the epidemic began
$\mathbb{S}_0$	Number of susceptible individuals at time t_0
$\mathbb{I}_0$	Number of infected individuals at time t_0
$\mathbb{U}_0$	Number of unreported individuates at time t_0
$\mathbb{R}_0$	Number of reported individuates at time t_0
$\mathscr{J}$	Rate of transmission at time t_0
$\frac{1}{\beta}$	Represents the average time during which asymptomatic infectious become asymptomatic
β_1	Rate at which asymptomatic infectious become reported symptomatic
β_2	Rate at which asymptomatic infectious become unreported symptomatic
$\frac{1}{\mu}$	Average time symptomatic infectious have symptoms

We follow the basic reproduction number ($\mathscr{R}_0$) of the model (3) is given in [31].

$$\mathscr{R}_0 = \left(\frac{\mathscr{J}_0 \mathbb{S}_0}{\beta_1 + \beta_2}\right)\left(1 + \frac{\beta_2}{\mu}\right) = \frac{\mathscr{J}_0 \mathbb{S}_0(\mu + \beta_2)}{\mu(\beta_1 + \beta_2)}. \tag{4}$$

The disease will decrease if $\mathscr{R}_0 < 1$. The disease will spread if $\mathscr{R}_0 > 1$ because every infection causes more than one new infection, see [31]. In this study, we consider $\mathscr{R}_0 > 1$.

4 Existence of the optimal control problem

In this section, we apply the optimal control theory to maximise the number of recovering people while lowering the number of infected individuals at the lowest possible cost and with the fewest possible unreported symptomatic infected population. Finally, we compute the numerical solution of the system and discuss the best control techniques using GL-NWAFDM.

Theorem 1 *We consider the optimal control system (3). There exists an OC* $\left(\mathscr{U}_l^*, \mathscr{U}_q^*, \mathscr{U}_s^*\right) \in \mathcal{U}$ *such as*

$$\mathcal{J}\left(\mathscr{U}_l^*, \mathscr{U}_q^*, \mathscr{U}_s^*\right) = \min_{\mathscr{U}_l, \mathscr{U}_q, \mathscr{U}_s \in \mathcal{U}} \mathcal{J}\left(\mathscr{U}_l, \mathscr{U}_q, \mathscr{U}_s\right). \tag{5}$$

Proof 1 *The existence of the OC can be investigated by using a result in [34]. The existence of the optimal control problem can be accomplished by checking the following steps:*

i. The corresponding state variables and the set of controls are nonempty. For this, we use a derived result of an existence in [35] to prove that the state variables and set of controls are nonempty. Let $\mathcal{Y}_j' = \mathcal{F}_{\mathcal{X}_i}(t, \mathcal{Y}_1, \mathcal{Y}_2, \mathcal{Y}_3, \mathcal{Y}_4)$, where $(\mathcal{Y}_1, \mathcal{Y}_2, \mathcal{Y}_3, \mathcal{Y}_4) = (\mathbb{S}, \mathbb{I}, \mathbb{U}, \mathbb{R})$. Let $\mathscr{U}_l, \mathscr{U}_q$ and $\mathcal{U}_s$ for some constants and $\mathcal{Y}_1, \mathcal{Y}_2, \mathcal{Y}_3$ and $\mathcal{Y}_4$ are continuous, then $\mathcal{F}_{\mathbb{S}}, \mathcal{F}_{\mathbb{I}}, \mathcal{F}_{\mathbb{U}}$ and $\mathcal{F}_{\mathbb{R}}$ are also continuous. Therefore, the state variables and set of controls are nonempty.

ii. Next, the control space $\mathcal{U} = \{(\mathscr{U}_l, \mathscr{U}_q, \mathscr{U}_s)/(\mathscr{U}_l, \mathscr{U}_q, \mathscr{U}_s)$ is measurable, $0 \le \mathscr{U}_{\min} \le \mathscr{U}_l \le \mathscr{U}_{\max} \le 1, 0 \le \mathscr{U}_{\min} \le \mathscr{U}_q \le \mathscr{U}_{\max} \le 1$,and $0 \le \mathscr{U}_{\min} \le \mathscr{U}_s \le \mathscr{U}_{\max} \le 1, t \in [0, \mathcal{T}_f - 1]\}$ is closed and convex.

iii. The right hand sides of the problem equations are bounded above by a sum of bounded state and controls and can be written as a linear function of $\mathscr{U}_l, \mathscr{U}_q$ and $\mathscr{U}_s$.

iv. The integrand in the objective functional, $\mathbb{I}(t) + \mathbb{U}(t) + \frac{\eta_1 \mathscr{U}_l^2(t)}{2} + \frac{\eta_2 \mathscr{U}_q^2(t)}{2} + \frac{\eta_3 \mathscr{U}_s^2(t)}{2}$ is convex on $\mathcal{U}$.

v. Finally, we show that there exists constants $\gamma_1, \gamma_2, \gamma_3, \gamma_4$ and γ such that $\mathbb{I}(t) + \mathbb{U}(t) + \frac{\eta_1 \mathscr{U}_l^2(t)}{2} + \frac{\eta_2 \mathscr{U}_q^2(t)}{2} + \frac{\eta_3 \mathscr{U}_s^2(t)}{2}$ satisfies $\mathbb{I}(t) + \mathbb{U}(t) + \frac{\eta_1 \mathscr{U}_l^2(t)}{2} + \frac{\eta_2 \mathscr{U}_q^2(t)}{2} + \frac{\eta_3 \mathscr{U}_s^2(t)}{2} \ge \gamma_1 + \gamma_2 |\mathscr{U}_l|^\gamma + \gamma_3 |\mathscr{U}_q|^\gamma + \gamma_4 |\mathscr{U}_s|^\gamma$. The state variables bounded, let $\gamma_1 = \inf_{t \in [0, \mathcal{T}_f]} (\mathbb{I}(t) + \mathbb{U}(t)), \gamma_2 = \frac{\eta_1}{2}, \gamma_3 = \frac{\eta_2}{2}, \gamma_4 = \frac{\eta_3}{2}$ and $\gamma = 2$ then it follows $\mathbb{I}(t) + \mathbb{U}(t) + \frac{\eta_1 \mathscr{U}_l^2(t)}{2} + \frac{\eta_2 \mathscr{U}_q^2(t)}{2} + \frac{\eta_3 \mathscr{U}_s^2(t)}{2} \ge \gamma_1 + \gamma_2 |\mathscr{U}_l|^\gamma + \gamma_3 |\mathscr{U}_q|^\gamma + \gamma_4 |\mathscr{U}_s|^\gamma$.

Hence, from Fleming et al. [34], the results indicate that there is an optimal control. Now, let system (3) in $\mathbb{R}^6$

$$\mathcal{U} = \left\{(\mathscr{U}_l(.), \mathscr{U}_q(.), \mathscr{U}_s(.)), 0 \le \mathscr{U}_l(.), \mathscr{U}_q(.), \mathscr{U}_s(.) \le 1, \forall t \in [0, \mathcal{T}_f]\right\},$$

where $\mathscr{U}_l, \mathscr{U}_q, \mathscr{U}_s$ are Lebesgue measurable on $[0,1]$. We define the objective functional as:

$$\mathcal{J}(\mathscr{U}_l, \mathscr{U}_q, \mathscr{U}_s) = \int_0^{\mathcal{T}_f} \left(\mathbb{I}(t) + \mathbb{U}(t) + \frac{\eta_1 \mathscr{U}_l^2(t)}{2} + \frac{\eta_2 \mathscr{U}_q^2(t)}{2} + \frac{\eta_3 \mathscr{U}_s^2(t)}{2}\right) dt. \tag{6}$$

The next step is to evaluate $\mathscr{U}_l, \mathscr{U}_q, \mathscr{U}_s$ as:

$$\mathcal{J}(\mathscr{U}_l, \mathscr{U}_q, \mathscr{U}_s) = \int_0^{\mathcal{T}_f} \mathscr{F}(\mathbb{S}, \mathbb{I}, \mathbb{R}, \mathbb{U}, \mathscr{U}_l, \mathscr{U}_q, \mathscr{U}_s, t) dt \tag{7}$$

is minimum, subject to restrictions

$${}_0^C D_t^\alpha \mathbb{W}_j = \chi_i, \tag{8}$$

where

$$\chi_i = \chi_i(\mathbb{S}, \mathbb{I}, \mathbb{R}, \mathbb{U}, \mathscr{U}_l, \mathscr{U}_q, \mathscr{U}_s, t), \qquad i = 1, \dots, 4,$$

$$\mathbb{W}_j = \{\mathbb{S}, \mathbb{I}, \mathbb{R}, \mathbb{U}, \qquad j = 1, \dots, 4\},$$

and the initial conditions satisfying

$$\mathbb{W}_1(t_0) = \mathbb{S}_0, \quad \mathbb{W}_2(t_0) = \mathbb{I}_0, \quad \mathbb{W}_3(t_0) = \mathbb{R}_0, \quad \mathbb{W}_4(t_0) = \mathbb{U}_0.$$

We use the fractional order case of the Pontryagin maximum principle, this fractional form is given by Agrawal in [26]. Functional modified as:

$$\bar{\mathcal{J}} = \int_{0}^{\mathcal{T}_f} \left[\mathcal{H}\left(\mathbb{S}, \mathbb{I}, \mathbb{R}, \mathbb{U}, \mathcal{U}_l, \mathcal{U}_q, \mathcal{U}_s, t\right) - \sum_{i=1}^{4} \mathcal{B}_i \chi_i \left(\mathbb{S}, \mathbb{I}, \mathbb{R}, \mathbb{U}, \mathcal{U}_l, \mathcal{U}_q, \mathcal{U}_s, t\right) \right] dt. \tag{9}$$

We define the Hamiltonian as:

$$\mathcal{H}\left(\mathbb{S}, \mathbb{I}, \mathbb{R}, \mathbb{U}, \mathcal{U}_l, \mathcal{U}_q, \mathcal{U}_s, t\right) = \mathcal{F}\left(\mathbb{S}, \mathbb{I}, \mathbb{R}, \mathbb{U}, \mathcal{U}_l, \mathcal{U}_q, \mathcal{U}_s, \mathcal{B}_i, t\right) + \sum_{i=1}^{4} \mathcal{B}_i \chi_i \left(\mathbb{S}, \mathbb{I}, \mathbb{R}, \mathbb{U}, \mathcal{U}_l, \mathcal{U}_q, \mathcal{U}_s, t\right). \tag{10}$$

We have got the necessary conditions from (9) and (10):

$${}_0^C D_t^{\alpha} \mathcal{B}_i = \frac{\partial \mathcal{H}}{\partial \mathcal{M}_i}, \ i = 1, ..., 4, \tag{11}$$

where $\mathcal{M}_i = \{\mathbb{S}, \mathbb{I}, \mathbb{R}, \mathbb{U}, \mathcal{U}_l, \mathcal{U}_q, \mathcal{U}_s, \mathcal{B}_i, t, i = 1, ..., 4\}$,

$$0 = \frac{\partial \mathcal{H}}{\partial \mathcal{U}_{\mathcal{K}}}, \ \mathcal{K} = l, q, s, \tag{12}$$

$${}_0^C D_t^{\alpha} \mathcal{M}_i = \frac{\partial \mathcal{H}}{\partial \mathcal{B}_i}, \ i = 1, ..., 4, \tag{13}$$

with

$$\mathcal{B}_i(\mathcal{T}_f) = 0, \ i = 1, ..., 4. \tag{14}$$

For more information, see [36].

Theorem 2 *The optimal control variables $\mathcal{U}_l, \mathcal{U}_q, \mathcal{U}_s$, with the corresponding solutions $\mathbb{S}^*, \mathbb{I}^*, \mathbb{R}^*, \mathbb{U}^*$ that minimize $\mathcal{J}(\mathcal{U}_l, \mathcal{U}_q, \mathcal{U}_s)$. There are also adjacent variables $\mathcal{B}_i$, $i = 1, ..., 4$ satisfying the following:*

- Adjoint equations:

$${}_0^C \mathcal{D}_t^{\alpha}[\mathcal{B}_1] = -\left(\left(1 - \mathcal{U}_l^*\right) \mathcal{J} \left[\mathbb{I}^* + \mathbb{U}^*\right]\right) \left(\mathcal{B}_1 + \mathcal{B}_2\right) - \mathcal{B}_1 \mathcal{U}_q^* - \mathcal{B}_3 \mathcal{U}_q^*, \tag{15}$$

$${}_0^C \mathcal{D}_t^{\alpha}]\mathcal{B}_2] = -1 + \left(1 - \mathcal{U}_l^*\right) \mathcal{J} \mathbb{S}^* \left(\mathcal{B}_1 - \mathcal{B}_2\right) + \mathcal{B}_2 \beta - \mathcal{B}_3 \beta_1 - \mathcal{B}_4 \beta_2, \tag{16}$$

$${}_0^C \mathcal{D}_t^{\alpha}[\mathcal{B}_3] = \mathcal{B}_3 \mu, \tag{17}$$

$${}_0^C \mathcal{D}_t^{\alpha}[\mathcal{B}_4] = -1 + \left(1 - \mathcal{U}_l^*\right) \mathcal{J} \mathbb{S}^* \left(\mathcal{B}_1 - \mathcal{B}_2\right) - \mathcal{U}_s^* \mathcal{B}_1 + \mathcal{B}_4 \left(\mu - \mathcal{U}_s^*\right). \tag{18}$$

- The transversality conditions:

$$\mathcal{B}_i(\mathcal{T}_f) = 0, \ i = 1, ..., 4. \tag{19}$$

- Optimality conditions:

$$\mathcal{H}\left(\mathbb{S}, \mathbb{I}, \mathbb{R}, \mathbb{U}, \mathcal{U}_l, \mathcal{U}_q, \mathcal{U}_s, \mathcal{B}_i, t\right) = \min_{0 \le \mathcal{U}_p, \mathcal{U}_{ap}, \mathcal{U}_{cp} \le 1} \mathcal{H}\left(\mathbb{S}, \mathbb{I}, \mathbb{R}, \mathbb{U}, \mathcal{U}_l, \mathcal{U}_q, \mathcal{U}_s, \mathcal{B}_i, t\right). \tag{20}$$

Further,

$$\mathcal{U}_l = \min\left\{1, \max\left\{0, \frac{\mathcal{J} \mathbb{S}^* \left[\mathbb{I}^* + \mathbb{U}^*\right] \left(\mathcal{B}_1 - \mathcal{B}_2\right)}{\eta_1}\right\}\right\}, \tag{21}$$

$$\mathcal{U}_q = \min\left\{1, \max\left\{0, \frac{\mathbb{S}^* \left(\mathcal{B}_1 - \mathcal{B}_3\right)}{\eta_2}\right\}\right\}, \tag{22}$$

$$\mathcal{U}_s = \min\left\{1, \max\left\{0, \frac{\mathbb{U}^* \left(\mathcal{B}_4 - \mathcal{B}_2\right)}{\eta_3}\right\}\right\}. \tag{23}$$

Proof 2 *Eq. (15) to Eq. (19) can be obtained from (11), where*

$$\mathcal{H}^* = \mathcal{B}_1{}_0^c\mathcal{D}_t^\alpha \mathbb{S}^* + \mathcal{B}_2{}_0^c\mathcal{D}_t^\alpha \mathbb{I}^* + \mathcal{B}_3{}_0^c\mathcal{D}_t^\alpha \mathbb{R}^* + \mathcal{B}_4{}_0^c\mathcal{D}_t^\alpha \mathbb{U}^* + \mathbb{I}^* + \mathbb{R}^* + \mathbb{U}^* + \frac{\eta_1 \mathcal{U}_l^2(t)}{2} + \frac{\eta_2 \mathcal{U}_q^2(t)}{2} + \frac{\eta_3 \mathcal{U}_s^2(t)}{2}$$

is the Hamiltonian. The conditions $\mathcal{B}_i(\mathcal{T}_f) = 0, i = 1, ..., 4$, hold. Now, using Eq. (20), we claim Eq. (21) to Eq. (23). Now, the state equations derived:

$$\begin{aligned}
{}_0^c\mathcal{D}_t^\alpha[\mathbb{S}] &= -\left(1-\mathcal{U}_l^*\right)\mathcal{J}(t)\mathbb{S}^*(t)\left[\mathbb{I}^*(t)+\mathbb{U}^*(t)\right] - \mathcal{U}_q^*\mathbb{S}^* + \mathcal{U}_s^*\mathbb{U}^*, && (24)\\
{}_0^c\mathcal{D}_t^\alpha[\mathbb{I}] &= \left(1-\mathcal{U}_l^*\right)\mathcal{J}(t)\mathbb{S}(t)^*\left[\mathbb{I}^*(t)+\mathbb{U}^*(t)\right] - \beta\mathbb{I}^*(t), && (25)\\
{}_0^c\mathcal{D}_t^\alpha[\mathbb{R}] &= \beta_1\mathbb{I}^*(t) - \mu\mathbb{R}^*(t) + \mathcal{U}_q^*\mathbb{S}^*, && (26)\\
{}_0^c\mathcal{D}_t^\alpha[\mathbb{U}] &= \beta_2\mathbb{I}^*(t) - \mu\mathbb{U}^*(t) - \mathcal{U}_s^*\mathbb{U}^*. && (27)
\end{aligned}$$

5 Procedure for solving control system

In this part of the paper, we develop a numerical scheme called GL-NWAFDM. Several results about this numerical scheme were discussed in [37, 38, 39]. The stability and efficiency of this method depend on the weight factor $0 \leq \Omega \leq 1$. Before, applying the GL-NWAFDM to the consider model, we first discrete the Caputo fractional derivative (2) by replacing $\triangle t$ by $\Psi(t)$, where

$$\Psi(\triangle t) = \triangle(t) + O(\triangle(t)^2), \quad 0 < \Psi(\triangle t) < 1, \quad \triangle(t) \to 0.$$

Then, the discretization for equations (24) to (27), where $\mathcal{K} = 0, 1, 2, ..., \mathcal{N}$, using GL-NWAFDM can be written as

$$\begin{aligned}
\mathbb{S}^{\mathcal{K}+1*} - \sum_{i=1}^{\mathcal{K}+1}\mu_i\mathbb{S}^{\mathcal{K}+1-i*} - \mathcal{Y}_{\mathcal{K}+1}\mathbb{S}^{0*} &= \Omega\Psi(\triangle t)^\alpha\left(-\left(1-\mathcal{U}_l^*\right)\mathcal{J}\mathbb{S}^{\mathcal{K}+1*}\left[\mathbb{I}^{\mathcal{K}+1*}+\mathbb{U}^{\mathcal{K}+1*}\right] - \mathcal{U}_q^{\mathcal{K}+1*}\mathbb{S}^{\mathcal{K}+1*} + \mathcal{U}_s^{\mathcal{K}+1*}\mathbb{U}^{\mathcal{K}+1*}\right)\\
&\quad + (1-\Omega)\Psi(\triangle t)^\alpha\left(-\left(1-\mathcal{U}_l^{\mathcal{K}*}\right)\mathcal{J}\mathbb{S}^{\mathcal{K}*}\left[\mathbb{I}^{\mathcal{K}*}+\mathbb{U}^{\mathcal{K}*}\right] + \left(-\mathcal{U}_q^{\mathcal{K}*}\mathbb{S}^{\mathcal{K}*} + \mathcal{U}_s^{\mathcal{K}*}\mathbb{U}^{\mathcal{K}*}\right)\right),
\end{aligned}$$

$$\begin{aligned}
\mathbb{I}^{\mathcal{K}+1*} - \sum_{i=1}^{\mathcal{K}+1*}u_i\mathbb{I}^{\mathcal{K}+1-i*} - \mathcal{Y}_{\mathcal{K}+1}\mathbb{I}^{0*} &= \Omega\Psi(\triangle t)^\alpha\left(\left(1-\mathcal{U}_l^{\mathcal{K}+1*}\right)\mathcal{J}\mathbb{S}^{\mathcal{K}+1*}\left[\mathbb{I}^{\mathcal{K}+1*}+\mathbb{U}^{\mathcal{K}+1*}\right] - \beta\mathbb{I}^{\mathcal{K}+1*}\right)\\
&\quad + (1-\Omega)\Psi(\triangle t)^\alpha\left(\left(1-\mathcal{U}_l^{\mathcal{K}*}\right)\mathcal{J}\mathbb{S}^{\mathcal{K}*}\left[\mathbb{I}^{\mathcal{K}*}+\mathbb{U}^{\mathcal{K}*}\right] - \beta\mathbb{I}^{\mathcal{K}*}\right),
\end{aligned}$$

$$\begin{aligned}
\mathbb{R}^{\mathcal{K}+1*} - \sum_{i=1}^{\mathcal{K}+1}u_i\mathbb{R}^{\mathcal{K}+1-i*} - \mathcal{Y}_{\mathcal{K}+1}1\mathbb{R}^{0*} &= \Omega\Psi(\triangle t)^\alpha\left(\beta_1\mathbb{I}^{\mathcal{K}+1*} - \mu\mathbb{R}^{\mathcal{K}+1*} + \mathcal{U}_q^{\mathcal{K}+1*}\mathbb{S}^{\mathcal{K}+1*}\right)\\
&\quad + (1-\Omega)\Psi(\triangle t)^\alpha\left(\beta_1\mathbb{I}^{\mathcal{K}*} - \mu\mathbb{R}^{\mathcal{K}*} + \mathcal{U}_q^{\mathcal{K}*}\mathbb{S}^{\mathcal{K}*}\right),
\end{aligned}$$

$$\begin{aligned}
\mathbb{U}^{\mathcal{K}+1*} - \sum_{i=1}^{\mathcal{K}+1}u_i\mathbb{U}^{\mathcal{K}+1-i*} - \mathcal{Y}_{\mathcal{K}+1}\mathbb{U}^{0*} &= \Omega\Psi(\triangle t)^\alpha\left(\beta_2\mathbb{I}^{\mathcal{K}+1*} - \mu\mathbb{U}^{\mathcal{K}+1*} - \mathcal{U}_s^{\mathcal{K}+1*}\mathbb{U}^{\mathcal{K}+1*}\right)\\
&\quad + (1-\Omega)\Psi(\triangle t)^\alpha\left(\beta_2\mathbb{I}^{\mathcal{K}*} - \mu\mathbb{U}^{\mathcal{K}*} - \mathcal{U}_s^{\mathcal{K}*}\mathbb{U}^{\mathcal{K}*}\right).
\end{aligned}$$

We observe that this method is partially implicit for $\Omega \in [0, 1]$ and fully implicit for $\Omega = 1$ and explicit when $\Omega = 0$.

6 Stability of the developed numerical scheme

This section is devoted to describe that the GL-NWAFDM is unconditionally stable in implicit cases ($0 < \Omega < 1$). The stability of the numerical scheme is checked when ($\Omega \neq 0$), for this need, we take the test problem of the linear fractional differential equation:

$${}_0^c\mathcal{D}_t^\alpha\mathcal{X}(t) = P\mathcal{X}(t)t > 0, 0 < \alpha \leq 1, P < 0. \tag{28}$$

Let the approximate solution of this equation is $\mathcal{X}(t_{\mathcal{K}}) = \mathcal{X}_{\mathcal{K}} = \mathcal{Z}_{\mathcal{K}}$, then applying the GL-NWAFDM, we rewrite Eq. (28) as

$$\mathcal{Z}^{\mathcal{K}+1} - \sum_{i=1}^{\mathcal{K}+1}\mu_i\mathcal{Z}^{\mathcal{K}+1-i} - \mathcal{Y}_{\mathcal{K}+1}\mathcal{Z}^0 = \Psi(\triangle t)^\alpha\left(\Omega P\mathcal{Z}^{\mathcal{K}+1} + (1-\Psi)P\mathcal{Z}^{\mathcal{K}}\right).$$

Then, we have

$$\mathcal{Z}^{\mathcal{K}+1} = \frac{1}{(1-\Psi(\triangle t)^\alpha\Omega P)}\left(\sum_{i=1}^{\mathcal{K}+1}\mu_i\mathcal{Z}^{\mathcal{K}+1-i} + \mathcal{Y}_{\mathcal{K}+1}\mathcal{Z}^0 + (1-\Psi)\Omega(\triangle t)^\alpha P\mathcal{Z}^{\mathcal{K}}\right), \qquad \mathcal{K} \geq 1,$$

we have $\frac{1}{(1-\Psi(\triangle t)^\alpha\Omega P)} < 1$, therefore, $\mathcal{Z}^1 \leq \mathcal{Z}^0$, $\mathcal{Z}^{\mathcal{K}+1} \leq \mathcal{Z}^{\mathcal{K}} \leq \mathcal{Z}^{\mathcal{K}-1} \leq ... \leq \mathcal{Z}^0$. Hence, the proposed numerical method is stable.

7 Graphical representation and discussion

In this part of the paper, we have presented the graphical representation of the system (3) with and without control variables. Gl-NWAFDM is used in the previous section to get the approximate solution of the modified model with the given initial conditions and parameters values: $\mathbb{S}(0) = 100$, $\mathbb{I}(0) = 900$, $\mathbb{R}(0) = 100$, $\mathbb{U}(0) = 900$ and different values of fractional parameter with $\beta_1 = 0.98$, $\beta_2 = 0.87$, $\mu = 0.432$, $\mathscr{F} = 0.218$ and $\beta = 0.098$.

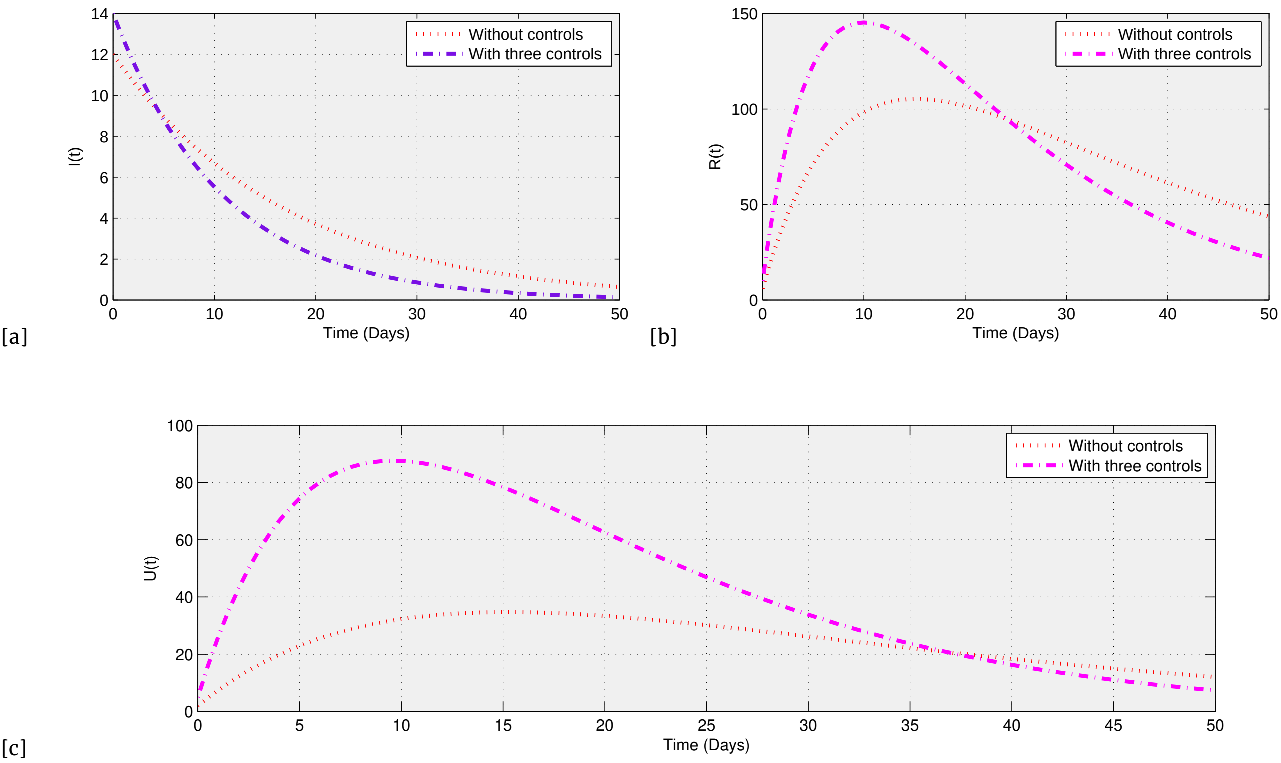

Figure 1. Simulations of $\mathbb{I}$,$\mathbb{R}$,and $\mathbb{U}$ at $\alpha = 0.85$ with and without controls

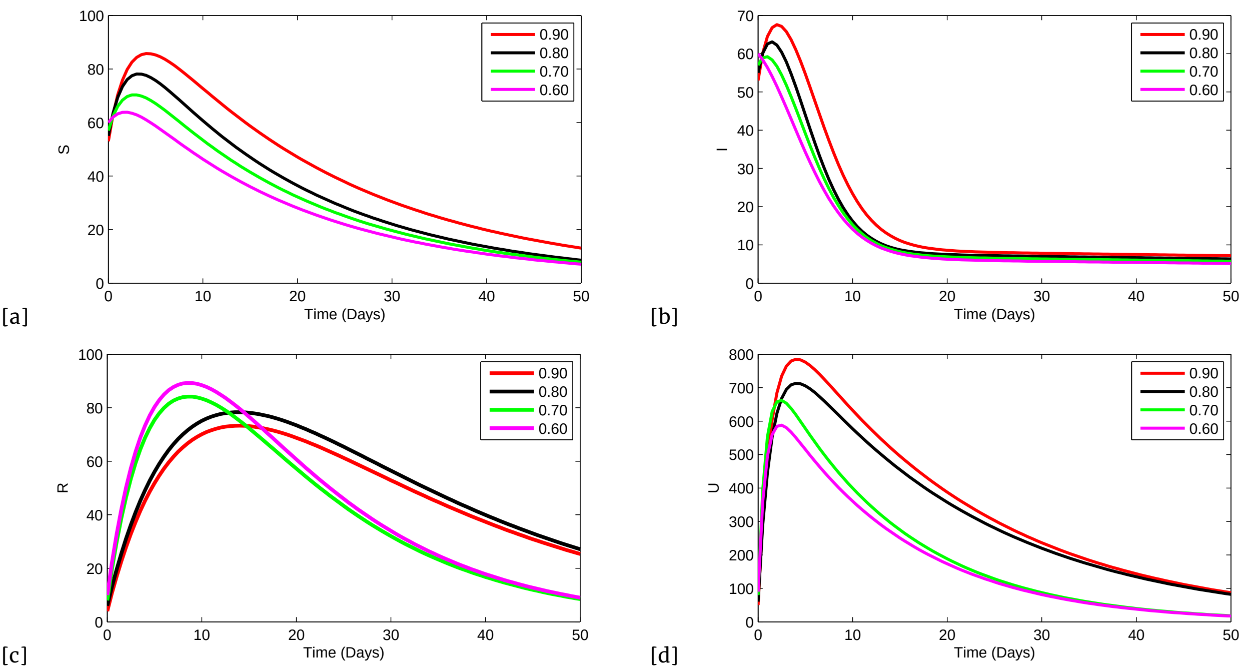

Figure 2. Numerical simulations of optimal control system with $\Omega = 10.23$ for $\alpha = 0.90, 0.80, 0.70$ and 0.60.

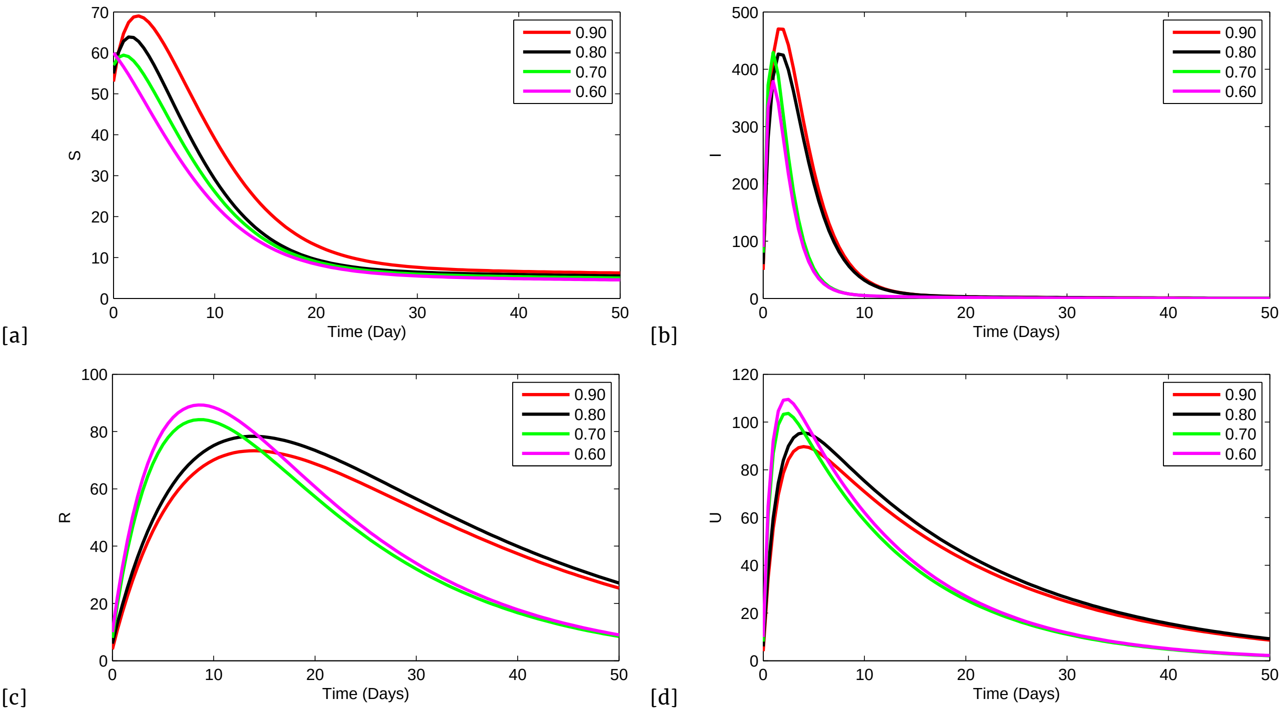

Figure 3. Numerical simulations of optimal control system with Ω = 11.32 for α = 0.90, 0.80, 0.70 and 0.60.

These figures show the efficiency and effectiveness of three control variables for the COVID-19 model. We have noted that the results obtained if Ω = 11.32 were fully implicit. Moreover, for the control case best result is given at α = 0.6. The dynamic of the solutions in the control case is shown in Figs. 2 and 3 by using various values of α and $\mathcal{T}_h$. These figures show that the approximate solutions of $\mathbb{S}$, $\mathbb{I}$, $\mathbb{R}$, $\mathbb{U}$ are unconditionally stable at Ω = 11.32. Fig. 3 shows that the peak values of each infected category of the population decreases significantly when fractional order decreases. $\mathbb{U}$ (Un-reported infected) starts with a decreasing slope and later changes the peak but with a small number of infected individuals. This describes that these classes can have a huge impact on the development of the reported infected graph.

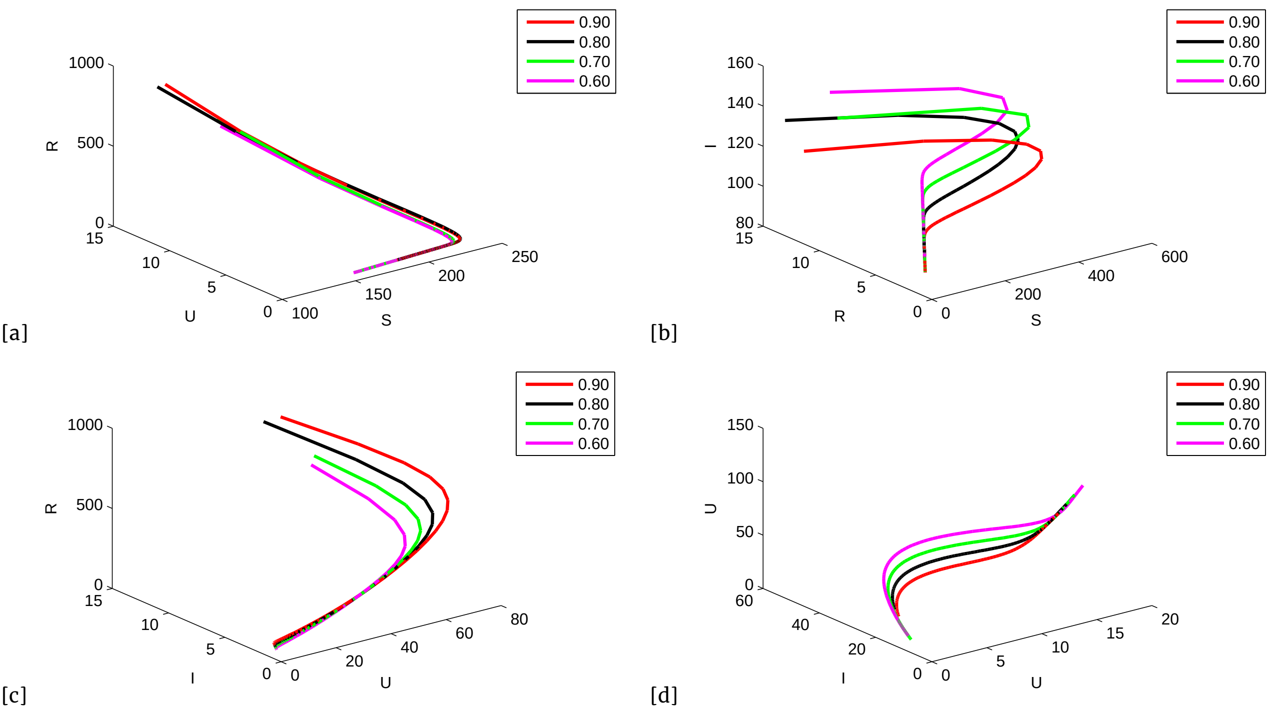

Figure 4. Numerical simulations of $\mathbb{I}$ with respect to $\mathbb{S}$, $\mathbb{R}$, and $\mathbb{U}$ with three controls variables for α = 0.90, 0.80, 0.70 and 0.60.

8 Conclusion

In this work, we have presented a novel coronavirus model with the combination of optimal control and fractional-order derivatives to increase the model complexity and to improve the model dynamics. We have added three control variables to health care such as, $\mathscr{U}_q$, $\mathscr{U}_s$, $\mathscr{U}_l$, (Quarantine, Self isolation, Lockdown). These OC variables have been used to decrease the number of the asymptotically infected and unreported infected as we can see in Figs. 2 and 3. For this need, we have derived the necessary optimality conditions. GL-NWAFDM has been developed to obtain the approximate solution of the proposed model. This numerical method depends on the values of the factor ω. Further, we have also proved the stability of the Gl-NWAFDM. Finally, graphical representations have been presented to support our theoretical results. We have concluded that the fractional optimality systems can be solved effectively by using the Gl-NWAFDM.

Declarations

Consent for publication

Not applicable.

Conflicts of interest

The authors declare that they have no conflict of interests.

Funding

This research received no specific grant from any funding agency in the public, commercial, or not-for-profit sectors.

Author's contributions

I.U.H.: Conceptualization, Methodology, Software, investigation, Writing - Original Draft, Data Curation, Formal Analysis. N.A.: Writing-Review & Editing, Supervision, Formal Analysis. K.S.N.: Software, Validation, Writing-Review & Editing, Project Administration. All authors discussed the results and contributed to the final manuscript.

Acknowledgements

Not applicable.

References

[1] Bashier, H., Khader, Y., Al-Souri, R., & Abu-Khader, I. A Novel Coronavirus Outbreak: A Teaching Case-Study. *The Pan African Medical Journal*, 36(11), (2020).

[2] Ndaïrou, F., Area, I., Nieto, J.J., & Torres, D.F. Mathematical modeling of COVID-19 transmission dynamics with a case study of Wuhan. *Chaos, Solitons & Fractals*, 135, 109846, (2020). [CrossRef]

[3] Khan, M.A., & Atangana, A. Modeling the dynamics of novel coronavirus (2019-nCov) with fractional derivative. *Alexandria Engineering Journal*, 59(4), 2379-2389, (2020). [CrossRef]

[4] Machado, J.A., & Lopes, A.M. Rare and extreme events: the case of COVID-19 pandemic. *Nonlinear dynamics*, 100(3), 2953-2972, (2020). [CrossRef]

[5] Chen, T.M., Rui, J., Wang, Q.P., Zhao, Z.Y., Cui, J.A., & Yin, L. A mathematical model for simulating the phase-based transmissibility of a novel coronavirus. *Infectious diseases of poverty*, 9(1), 1-8, (2020). [CrossRef]

[6] Ivorra, B., Ferrández, M.R., Vela-Pérez, M., & Ramos, A.M. Mathematical modeling of the spread of the coronavirus disease 2019 (COVID-19) taking into account the undetected infections. The case of China. *Communications in nonlinear science and numerical simulation*, 88, 105303, (2020). [CrossRef]

[7] Naik, P.A., Yavuz, M., Qureshi, S., Zu, J., & Townley, S. Modeling and analysis of COVID-19 epidemics with treatment in fractional derivatives using real data from Pakistan. *The European Physical Journal Plus*, 135(10), 1-42, (2020). [CrossRef]

[8] Allegretti, S., Bulai, I.M., Marino, R., Menandro, M.A., & Parisi, K. Vaccination effect conjoint to fraction of avoided contacts for a Sars-Cov-2 mathematical model. *Mathematical Modelling and Numerical Simulation with Applications*, 1(2), 56-66, (2021). [CrossRef]

[9] Özköse, F., Yavuz, M., Şenel, M.T., & Habbireeh, R. Fractional order modelling of omicron SARS-CoV-2 variant containing heart attack effect using real data from the United Kingdom. *Chaos, Solitons & Fractals*, 157, 111954, (2022). [CrossRef]

[10] Dietz, K., & Heesterbeek, J.A.P. Bernoulli was ahead of modern epidemiology. *Nature*, 408(6812), 513-514, (2000). [CrossRef]

[11] Khan, H., Gómez-Aguilar, J.F., Alkhazzan, A., & Khan, A. A fractional order HIV-TB coinfection model with nonsingular Mittag-Leffler Law. *Mathematical Methods in the Applied Sciences*, 43(6), 3786-3806, (2020). [CrossRef]

[12] Sweilam, N.H., Al-Mekhlafi, S.M., & Hassan, A.N. Numerical treatment for solving the fractional two-group influenza model. *Progress in Fractional Differentiation and Applications*, 4, 1-15, (2018).

[13] Kumar, S., Ghosh, S., Lotayif, M. S., & Samet, B. A model for describing the velocity of a particle in Brownian motion by Robotnov function based fractional operator. *Alexandria Engineering Journal*, 59(3), 1435-1449, (2020). [CrossRef]

[14] Rihan, F.A., Baleanu, D., Lakshmanan, S., & Rakkiyappan, R. On fractional SIRC model with salmonella bacterial infection. *Abstract and Applied Analysis*, (2014). [CrossRef]

[15] Hammouch, Z., Yavuz, M., & Özdemir, N. Numerical solutions and synchronization of a variable-order fractional chaotic system. *Mathematical Modelling and Numerical Simulation with Applications*, 1(1), 11-23, (2021). [CrossRef]

[16] Özköse, F., Şenel, M.T., & Habbireeh, R. Fractional-order mathematical modelling of cancer cells-cancer stem cells-immune system interaction with chemotherapy. *Mathematical Modelling and Numerical Simulation with Applications*, 1(2), 67-83, (2021). [CrossRef]
[17] Kostylenko, O., Rodrigues, H.S., & Torres, D.F. The risk of contagion spreading and its optimal control in the economy. *arXiv preprint arXiv:1812.06975*, (2018). [CrossRef]
[18] Lemos-Paião, A.P., Silva, C.J., Torres, D.F., & Venturino, E. Optimal control of aquatic diseases: A case study of Yemen's cholera outbreak. *Journal of Optimization Theory and Applications*, 185(3), 1008-1030, (2020). [CrossRef]
[19] Ammi, M.R.S., & Torres, D.F. Optimal control of a nonlocal thermistor problem with ABC fractional time derivatives. *Computers & Mathematics with Applications*, 78(5), 1507-1516, (2019). [CrossRef]
[20] Brandeau, M.L., Zaric, G.S., & Richter, A. Resource allocation for control of infectious diseases in multiple independent populations: beyond cost-effectiveness analysis. *Journal of health economics*, 22(4), 575-598, (2003). [CrossRef]
[21] Ball, F., & Becker, N.G. Control of transmission with two types of infection. *Mathematical biosciences*, 200(2), 170-187, (2006). [CrossRef]
[22] Castilho, C. Optimal control of an epidemic through educational campaigns. *Electronic Journal of Differential Equations (EJDE)[electronic only]*, 2006, Paper-No, (2006).
[23] Rihan, F.A., Lakshmanan, S., & Maurer, H. Optimal control of tumour-immune model with time-delay and immuno-chemotherapy. *Applied Mathematics and Computation*, 353, 147-165, (2019). [CrossRef]
[24] Sweilam, N., Rihan, F., & Seham, A.M. A fractional-order delay differential model with optimal control for cancer treatment based on synergy between anti-angiogenic and immune cell therapies. *Discrete & Continuous Dynamical Systems-S*, 13(9), 2403, (2020). [CrossRef]
[25] Zaky, M.A., & Machado, J.T. On the formulation and numerical simulation of distributed-order fractional optimal control problems. *Communications in Nonlinear Science and Numerical Simulation*, 52, 177-189, (2017). [CrossRef]
[26] Agrawal, O.P. A formulation and a numerical scheme for fractional optimal control problems. *IFAC Proceedings Volumes*, 39(11), 68-72, (2006). [CrossRef]
[27] Agrawal, O.P., Defterli, O., & Baleanu, D. Fractional optimal control problems with several state and control variables. *Journal of Vibration and Control*, 16(13), 1967-1976, (2010). [CrossRef]
[28] Sweilam, N.H., Al-Mekhlafi, S.M., & Baleanu, D. Optimal control for a fractional tuberculosis infection model including the impact of diabetes and resistant strains. *Journal of advanced research*, 17, 125-137, (2019). [CrossRef]
[29] Sweilam, N.H., Al-Mekhlafi, S.M., Alshomrani, A.S., & Baleanu, D. Comparative study for optimal control nonlinear variable-order fractional tumor model. *Chaos, Solitons & Fractals*, 136, 109810, (2020). [CrossRef]
[30] Sweilam, N.H., & AL–Mekhlafi, S.M. Optimal control for a time delay multi-strain tuberculosis fractional model: a numerical approach. *IMA Journal of Mathematical Control and Information*, 36(1), 317-340, (2019). [CrossRef]
[31] Liu, Z., Magal, P., Seydi, O., & Webb, G. Predicting the cumulative number of cases for the COVID-19 epidemic in China from early data. *arXiv preprint arXiv:2002.12298*, (2020). [CrossRef]
[32] Lakshmikantham, V., & Vatsala, A.S. Basic theory of fractional differential equations. *Nonlinear Analysis: Theory, Methods & Applications*, 69(8), 2677-2682, (2008). [CrossRef]
[33] Arenas, A.J., Gonzalez-Parra, G., & Chen-Charpentier, B.M. Construction of nonstandard finite difference schemes for the SI and SIR epidemic models of fractional order. *Mathematics and Computers in Simulation*, 121, 48-63, (2016). [CrossRef]
[34] Heimann, B., Fleming, W.H., Rishel, R.W., Deterministic and Stochastic Optimal Control. New York-Heidelberg-Berlin. Springer-Verlag. 1975. XIII, 222 S, DM 60, 60. *Zeitschrift Angewandte Mathematik und Mechanik*, 59(9), 494-494, (1979). [CrossRef]
[35] Kouidere, A., Youssoufi, L.E., Ferjouchia, H., Balatif, O., & Rachik, M. Optimal control of mathematical modeling of the spread of the COVID-19 pandemic with highlighting the negative impact of quarantine on diabetics people with cost-effectiveness. *Chaos, Solitons & Fractals*, 145, 110777, (2021). [CrossRef]
[36] Sweilam, N.H., Al-Ajami, T.M., & Hoppe, R.H. Numerical solution of some types of fractional optimal control problems. *The Scientific World Journal*, 2013, (2013). [CrossRef]
[37] Scherer, R., Kalla, S.L., Tang, Y., & Huang, J. The Grünwald–Letnikov method for fractional differential equations. *Computers & Mathematics with Applications*, 62(3), 902-917, (2011). [CrossRef]
[38] Li, L., & Wang, D. Numerical stability of Grünwald–Letnikov method for time fractional delay differential equations. *BIT Numerical Mathematics*, 1-33, (2021). [CrossRef]
[39] Chakraborty, M., Maiti, D., Konar, A., & Janarthanan, R. A study of the grunwald-letnikov definition for minimizing the effects of random noise on fractional order differential equations. In *2008 4th International Conference on Information and Automation for Sustainability*, 449-456, IEEE, (2008). [CrossRef]